

# Establishment and characterization of clinically relevant models of ependymoma: a true challenge for targeted therapy

Su Guan, Ruijun Shen, Tiffany Lafortune, Ningyi Tiao, Peter Houghton, W.K. Alfred Yung, and Dimpy Koul

*Brain Tumor Center, Department of Neuro-Oncology, The University of Texas MD Anderson Cancer Center, Houston, Texas (S.G., R.S., T.L., N.T., W.K.A.Y., D.K.); Center for Childhood Cancer, Nationwide Children's Hospital, Columbus, Ohio (P.H.)*

The development of new therapies for ependymoma is dramatically limited by the absence of optimal *in vivo* and *in vitro* models. Successful ependymoma treatment requires a profound understanding of the disease's biological characteristics. This study focuses on the establishment and characterization of *in vivo* and *in vitro* models of ependymoma to study the molecular pathways necessary for growth and progression in ependymoma. In addition, this study also emphasizes the use of these models for therapeutic intervention of ependymomas. We established optimal conditions for the long-term growth of 2 tumor xenografts and cultures of 2 human ependymoma cell lines. This study also describes the establishment of *in vivo* models. Histopathologic features of tumors from both intracranial and subcutaneous sites in mice revealed perivascular pseudorosettes and ependymal rosettes, which are typical morphologic features of ependymoma similar to those observed in human specimens. The *in vitro* models revealed glial fibrillary acidic protein and vimentin expression, and ultrastructural studies demonstrated numerous microvilli, caveolae, and microfilaments commonly seen in human ependymoma. To study signaling pathway alterations in ependymoma, we profiled established ependymoma models with Western blot analysis that demonstrated aberrant activation mainly of the phosphoinositide 3-kinase and epidermal growth factor receptor signaling pathways. Targeting phosphoinositide 3-kinase and epidermal growth factor receptor signaling pathways with small molecule inhibitors showed growth inhibitory effects.

These models can also be used to study the standard therapies used for ependymomas, as shown by some of the drugs used in this study. Therefore, the models developed will assist in the biological studies and preclinical drug screening for ependymomas.

**Keywords:** ependymoma, *in vitro*, *in vivo*, model, targeted therapy.

Ependymomas are rare gliomas of neuroectodermal origin that exhibit degrees of ependymal differentiation. They arise from ependymal cells in the obliterated central canal of the spinal cord, filum terminale, choroid plexus, or white matter adjacent to a highly angulated ventricular surface.<sup>1</sup> Ependymomas account for only 4%–8% of glioma cases but are the third most common central nervous system (CNS) tumor of childhood after astrocytomas (including pilocytic astrocytomas) and embryonal tumors (including medulloblastomas). They account for 2.1% of all primary brain tumors, regardless of patient age, for 6.4% of those in patients aged 1–14 years, and for 5% of those in patients aged 15–19 years.<sup>2</sup> The World Health Organization (WHO) classification of nervous system tumors recognizes 4 major subgroups of ependymal tumors: subependymoma (grade I), myxopapillary ependymoma (grade I), ependymoma (grade II), and anaplastic ependymoma (grade III).<sup>2</sup> The last of these seems to demonstrate more aggressive clinical behavior, although its diagnosis is subjective, and its prognostic significance remains controversial.<sup>3–8</sup>

From a clinical and biological perspective, intracranial ependymomas of childhood are enigmatic and challenging tumors to treat. Histologic features of anaplasia, such as mitoses, microvascular proliferation, and necrosis, serve as indicators of biological behavior in other gliomas; thus, their significance remains unclear in ependymoma.

Received October 12, 2010; accepted March 7, 2011.

Corresponding Author: Dimpy Koul, Department of Neuro-Oncology, Unit 100, The University of Texas MD Anderson Cancer Center, 1515 Holcombe Boulevard, Houston, TX 77030 (dkoul@mdanderson.org).

Ependymomas are widely considered to be a “surgical disease,” but a significant proportion of patients experience relapse even after complete surgical removal of the tumor. Pediatric ependymomas often arise infratentorially, filling in the fourth ventricle and extending into the brain stem;<sup>9</sup> thus, total removal of the tumor is rarely possible. In children with intracranial ependymomas, the 5-year event-free survival rate is <50%.<sup>3-6,10</sup> Although postoperative radiation therapy may result in long-term survival, radiation therapy-associated toxicities, such as retardation in physical and mental development,<sup>11</sup> prevent the wide application of radiation therapy in young patients. In addition, the effectiveness of postoperative chemotherapy is uncertain because these tumors are chemoresistant.<sup>12</sup>

Attempts to determine the optimum adjuvant treatment have been hindered by the relatively low incidence of the disease and the paucity of definitive clinical trials.<sup>3</sup> A lack of consensus regarding the prognostic value of histologic grading and a poor understanding of the disease’s biological characteristics have compounded this situation further.<sup>3,7</sup> Thus, more-effective treatment regimens depend almost entirely on a better understanding of the biological characteristics of these tumors. The development of agents with novel antineoplastic action is urgently needed, but progress is limited by the absence of optimal *in vivo* and *in vitro* models. As an approach to overcoming the limitations in childhood cancer drug development, several groups in the pediatric cancer community have systematically tested the validity of preclinical human tumor xenograft models to identify novel agents that may have clinical activity in childhood cancers.<sup>13-17</sup> There have been efforts toward development of clinically relevant models of ependymoma, and Yu et al<sup>18</sup> recently have been successful in establishment of an orthotopic ependymoma xenograft mouse model from a fresh surgical specimen of a recurrent anaplastic ependymoma. In addition Yu and colleagues also tested whether xenograft tumor cells can be maintained *in vitro* long term to establish a cell line. In this study, we describe the establishment of *in vivo* and *in vitro* models of ependymoma from human ependymomas. We determined the tumorigenicity and evaluated the clinical relevance by histopathological features of both intracranial and subcutaneous tumors. The cell lines generated were examined for the ependymal markers and ultrastructural features of ependymoma. To determine the molecular pathways necessary for tumor growth and progression and to test novel therapeutic approaches for ependymoma, signal profiles were obtained from *in vitro* model systems. On the basis of the alterations observed, we tested a few small molecule inhibitors of signaling pathways using *in vitro* model systems in growth assays.

## Material and Methods

### *Tumor Samples*

Two human xenograft tissue specimens were obtained from St. Jude Children’s Hospital (Memphis, TN): an

anaplastic ependymoma from the posterior fossa of a 2-year-old girl (BT-44) and a focally anaplastic ependymoma from the posterior fossa of a 10-month-old boy (BT-57). Tumor grade was determined by light microscopy in accordance with the 2007 WHO classification system.<sup>2</sup>

### *Subcutaneous and Intracranial Transplantations*

All animal experiments were conducted in accordance with protocols approved by The University of Texas M. D. Anderson Cancer Center (Houston, TX) Institutional Animal Care and Use Committee. Heterotopic tumor propagation was performed by implanting minced tissue into the flanks of 5–6-week-old athymic nu/nu mice. Tumor growth was monitored twice per week by palpation, and tumor diameters were measured using vernier calipers. Tumor volume was calculated on the basis of the assumption that the tumors were ellipsoid. Established tumors were resected and either fixed in 4% paraformaldehyde or flash-frozen in liquid nitrogen for histological evaluation and immunostaining or protein collection, respectively. To develop an intracranial disease model, we engrafted minced tumor tissue or a cell suspension of 1 million cells into the caudate nuclei of athymic mice using a previously described guide-screw system.<sup>19</sup> Animals were monitored daily until they developed signs of neurological deficit or became moribund, at which time they were euthanized and their brains removed for histopathological analysis.

### *In vitro Models*

*In vitro* models were created by directly cutting tumor fragments into small pieces using a scalpel blade and mechanical disruption by repetitive pipetting to make the cell suspension. The cell suspension was suspended in Dulbecco’s modified Eagle’s medium/F12 (Mediatech) containing 10% fetal bovine serum and antibiotics (100 U of penicillin and 50 µg/mL streptomycin) and plated on a poly-D-lysine-coated flask (25 cm<sup>2</sup>; BD Biocoat; Becton Dickinson), which facilitated cell attachment. Cultures were maintained in a 5% CO<sub>2</sub> and 95% humidified atmosphere. Additional growth factors such as 10 ng/mL epidermal growth factor (EGF; Millipore) and 10 ng/mL basic fibroblast growth factor (Invitrogen) were added to accelerate cell growth. Tumor propagation was performed by intracranially and subcutaneously inoculating mice with cells and/or with minced tumor tissues.

### *Tissue Processing and Immunohistochemistry*

For histopathologic studies, tissue sections were stained with hematoxylin and eosin. In brief, tumor sections were deparaffinized and rehydrated using xylene and gradient ethanol. The slides were stained with hematoxylin and eosin and mounted using Permount (Fisher Scientific).

Immunohistochemical analysis was performed to determine proliferative marker Ki-67 expression in both intracranial and subcutaneous xenograft samples. Paraffin-embedded tumor tissue sections were deparaffinized with xylene and rehydrated. Antigenic retrieval was performed by submerging the sample in 1× target solution (S1699; Dako) and steaming it at 95°C for 20 min. The sections were then treated with 3% hydrogen peroxide in methanol to quench endogenous peroxidase activity, followed by incubation with 1% goat serum to block nonspecific binding. The sections were then stained with anti-Ki-67 antibody (Santa Cruz Biotechnology)<sup>20</sup> overnight at 4°C. The tissue sections were incubated with the biotinylated anti-rabbit secondary antibody followed by further incubation with streptavidin-horseradish-peroxidase complex. They were then immersed in 3,3'-diaminobenzidine solution (Sigma Fast, D4418; Sigma-Aldrich) and mounted using Permount. For the negative control, the primary antibody was replaced by the nonimmune rabbit immunoglobulin of the same isotype. The distribution of Ki-67 was scored as negative (if <10% of cells yielded positive results) or positive (if ≥10% of cells yielded positive results).

#### *Immunofluorescence Assay*

Cells were seeded at a concentration of  $2 \times 10^5$  cells per well in 6-well plates with coverslips inside and left overnight. The following day, the cells were washed with phosphate-buffered saline (PBS) once before being fixed with 4% formaldehyde in PBS for 20 min. After another PBS wash, the cells were permeabilized with 0.1% Triton X-100 in PBS for 5 min and then blocked with 5% bovine serum albumin-0.1% Tween 20-PBS for 1 h. Cells were then incubated with mouse primary antibodies against glial fibrillary acidic protein (GFAP; anti-GFAP; Dako) and vimentin (anti-vimentin; Biomed<sup>21</sup>) for 1 h. After 2 washes with PBS (containing 0.1% Tween 20), the cells were incubated with the secondary antibodies conjugated with fluorescein isothiocyanate or Texas red (red fluorescence) for 1 h. Coverslips were mounted in Vecta-shield mounting medium containing DAPI (Vector Labs), and labeled cells were evaluated using fluorescent microscopy (Zeiss Axiovert 200; Carl Zeiss MicroImaging), with separate filters used for each fluorochrome. Images were obtained using the software package XCAP-Lite, version 2.1 (EPIX).

#### *Transmission Electron Microscopy*

Transmission electron microscopy was used to determine the ultrastructure of a single ependymoma cell. Samples were fixed with a solution containing 3% glutaraldehyde plus 2% paraformaldehyde in 0.1 M cacodylate buffer (pH 7.3) for 1 h. The samples were then washed and treated with 0.1% Millipore-filtered cacodylate-buffered tannic acid, postfixed with 1% buffered osmiumtetroxide for 30 min, and stained en bloc

with 1% Millipore-filtered uranylacetate. The samples were dehydrated in increasing concentrations of ethanol, infiltrated, and embedded in LX-112 medium. The samples were polymerized in a 70°C oven for 2 days. Ultrathin sections were cut using a Leica Ultracut microtome, stained with uranyl acetate and lead citrate in a Leica EM stainer, and evaluated using a JEM 1010 transmission electron microscope (JEOL) at an accelerating voltage of 80 kV. Digital images were obtained using the AMT Imaging System (Advanced Microscopy).

#### *Western Blot Analysis*

To identify the molecular signaling patterns altered in ependymoma, we profiled 2 established in vitro models using Western blot analysis. Total protein lysate was analyzed using Western blotting, as described previously.<sup>22</sup> In addition, lysis buffer was used to lyse mice xenografts by homogenization. Tumor lysates and cell lines lysates were probed with the following primary antibodies: phosphorylated or total Akt, P70S6, S6, PTEN, EGFR, Erb-2, Erb-3, and STAT-3 (Cell Signaling Technology). Blots were reprobed with a monoclonal antibody for b-actin (EMD Biosciences) as a control for protein loading.

#### *Cell Proliferation Assay*

On the basis of the alteration of the signaling pathway, we treated cells with PX866, NVP-BE235 (phosphoinositide-3 kinase [PI3K] inhibitors) and erlotinib (EGFR inhibitor) for 72 h. In addition, standard chemotherapies using temozolomide and carboplatin were also used in cell growth assays. Growth inhibition was determined using the CellTiter-Blue (Promega) viability assay. The half-maximal inhibitor concentration ( $IC_{50}$ ) value was calculated as the mean drug concentration required to inhibit cell proliferation by 50% compared with vehicle controls.<sup>23</sup>

## Results

### *Establishment of in vivo Ependymoma Model in Nude Mice*

To generate intracranial and subcutaneous models of ependymoma, 2 human xenografts, BT-44 and BT-57, were used. For the subcutaneous model, we injected either a single-cell suspension generated from mechanical disruption or minced tumor into the right and left flanks of nu/nu mice. Mice were observed for tumor growth over a period of time, and both BT-44 and BT-57 formed tumors in vivo. Tumors were measured twice per week and growth curves were generated measuring tumor volume versus days. The subcutaneous tumor growth rate for the cell lines were similar, and both BT-44 and BT-57 models revealed exponential

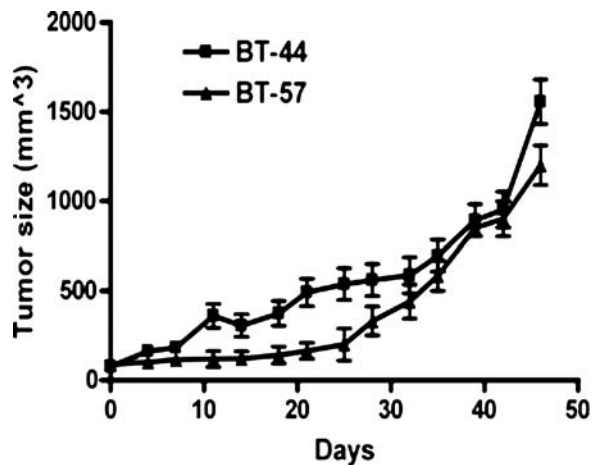


Fig. 1. Establishment of a subcutaneous ependymoma model. Tumor volumes were measured twice per week during the course of the experiment. After 40–50 days, exponential growth of the tumor mass was observed in the subcutaneous model.

growth of the tumor mass and formed significant tumors over a period of 40–50 days (Fig. 1).

For the intracranial model, human xenograft tissue specimens were minced into a single-cell suspension and injected into the caudate nucleus of athymic mice using a previously described guide-screw system.<sup>22</sup> All of the mice injected with tumor cells developed signs of neurological deficit or became moribund within 100–150 days after the injection. At that time point, animals were killed, and animal brains after sectioning were invariably enlarged and revealed huge tumor mass. Histopathological examination of the tumor revealed the typical phenotype of ependymoma, which displayed pseudorosette formation (Fig. 2A and 2B). These pseudorosettes revealed perivascular growth, and high cellularity confirmed typical ependymoma formation *in vivo*. In addition, the histopathological examination of the xenografts clearly showed grade 111 anaplastic ependymoma tumors with abundant mitosis. The immunohistochemical studies revealed a high proliferative rate of the tumors, as shown by high staining for the mitotic marker Ki-67. The paraffin-embedded sections of mouse brain tissue revealed intracranial tumors and tumor invasion into the brain parenchyma. Figure 2C shows the growth pattern in the BT-57 tumor; similar results were observed for the BT-44 tumor (results not shown). We did observe higher Ki-67 expression on intracranial tumors than in subcutaneous tumors, and a higher Ki-67 index in intracranial tumors than in subcutaneous tumors suggested that changes in tumor microenvironmental factors influence tumor growth, affecting growth rates differently depending on tumor location.

To achieve the goal of maintaining the tumor model, we used subtransplantation of xenograft tumors by harvesting the tumor cells from both subcutaneous and intracranial tumors and reinjecting them back in to the mice to develop the tumors again. The

subtransplantation procedure developed the tumors that displayed pseudorosette formation—a typical feature of ependymoma (Fig. 2D). The subtransplanted tumors had the same growth pattern as that of the initial passage, showing that repeated transplantations do not change the growth pattern of the tumor.

#### *Establishment of in vitro Ependymoma Models*

Two *in vitro* ependymoma models, BT-44 and BT-57, were established (Fig. 3A) using human xenografts. The morphologic characteristics of ependymoma cells varied, but most of the cells were spindle-like; others were round or oval, some were round to oval, and some were irregular. These cells could be passaged serially for 15–20 passages before the cells underwent senescence.

To characterize the established models for ependymal features, we performed immunofluorescence staining using anti-GFAP and vimentin antibodies. GFAP is an intermediate filament protein specific for astrocytes in the CNS and is expressed by other cell types, as well as in CNS ependymal cells. Both models (BT-44 and BT-57) stained positive for GFAP and vimentin in the cytoplasm (Fig. 3B). We also performed an ultrastructure study using electron microscopy, revealing identical structures in cultured models, including numerous microvilli on the plasma membranes and numerous caveolae, which are synthesized in the Golgi apparatus and dispersed in the cytoplasm. Numerous microfilaments, the ultrastructural feature of ependymoma cells, mitochondria, and microtubules, were widely distributed in the cytoplasm (Fig. 3C). The endoplasmic reticula were granular (which reflects the synthetic activity of tumor cells), filled with homogeneous material and clusters of free ribosomes, and widely distributed in the cytoplasm. The nuclei had a regular oval shape and contained evenly dispersed chromatin; they were located in the center of the cells and occupied a large portion of the cell volume.

#### *Molecular Signaling Alterations in Ependymoma*

To determine molecular signaling alterations in ependymoma, we profiled the 2 established models using Western blot analysis and probed them with various signaling pathway antibodies. Here, we aim to characterize the molecular signaling pattern altered in established ependymoma models and to target the altered signaling pathways with small molecule inhibitors. Our analysis indicated that ependymoma models derived from individual tumors exhibited divergent patterns of signaling pathway activation. Results indicated development of alterations of PI3K/Akt and EGFR pathways shown by activated Akt, S6K1, pS6, and EGFR levels in the ependymoma cell lines (Fig. 4A). We therefore tested the growth-inhibitory effect of PI3 Kinase inhibitors (NVP-BEZ235 and PX866) and an EGFR inhibitor (erlotinib) on ependymoma models using a CellTiter-Blue (CTB) growth assay (Fig. 5A). Treatment of BT-44 and

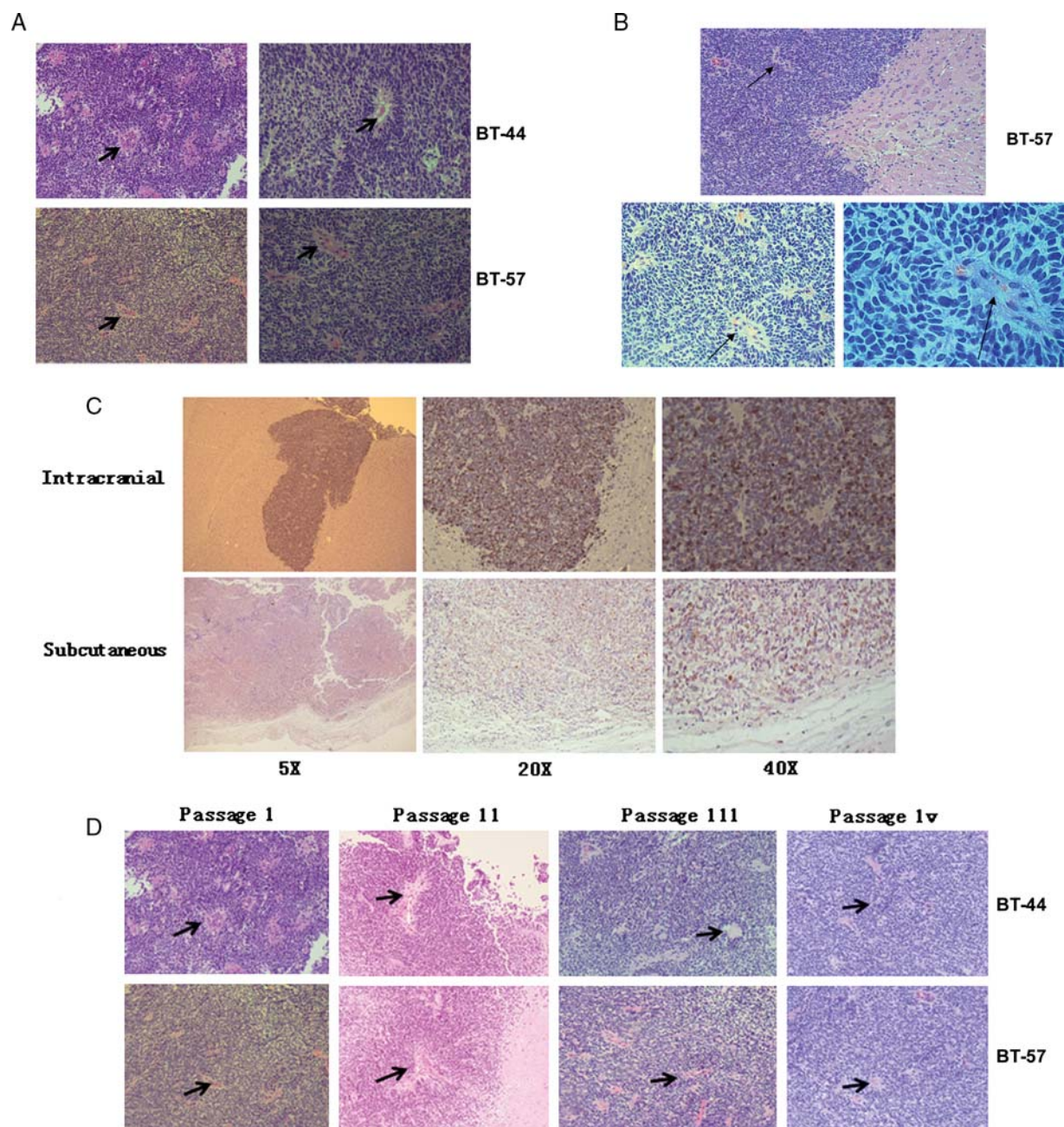


Fig. 2. Ependymoma marker detection in an in vivo model. (A) Subcutaneous xenograft models (top, BT-44; bottom, BT-57) revealed pseudorosette formation, a typical histological feature, as determined by hematoxylin and eosin staining. (B) Pseudorosettes were visible in intracranial tumors. (C) In vivo models were highly proliferative. Relatively high Ki-67 expression was observed in subcutaneous models (BT-57), and high expression was seen in intracranial tumors and tumors that had invaded into the brain parenchyma (BT-57). (D) Ependymoma xenografts in mouse brain. Hematoxylin and eosin staining showed maintenance of tumor phenotype after 4 repeated transplantations.

BT-57 cell lines with different signaling inhibitors for 72 h resulted in dose-dependent growth inhibition although the magnitude of the growth inhibition varied with IC<sub>50</sub> values in the low millimolar range (2–4 mM) for PX866 and nanomolar (5–10 nM) range for NVP-BE235. The IC<sub>50</sub> for the EGFR inhibitor erlotinib was ~10 μM for both models. Although we did observe an increase in PI3K-mediated signaling in these models,

the sensitivity toward PI3K inhibition indicates that cells with activated PI3K may respond better to these signaling inhibitors. Therefore, these findings suggest that targeted therapy may be an effective strategy for ependymoma.

In addition, we also determined the effects of standard chemotherapeutic drugs (eg, temozolomide and carboplatin) on ependymoma cell proliferation. The proliferation of BT-44 and BT-57 cells was decreased in a

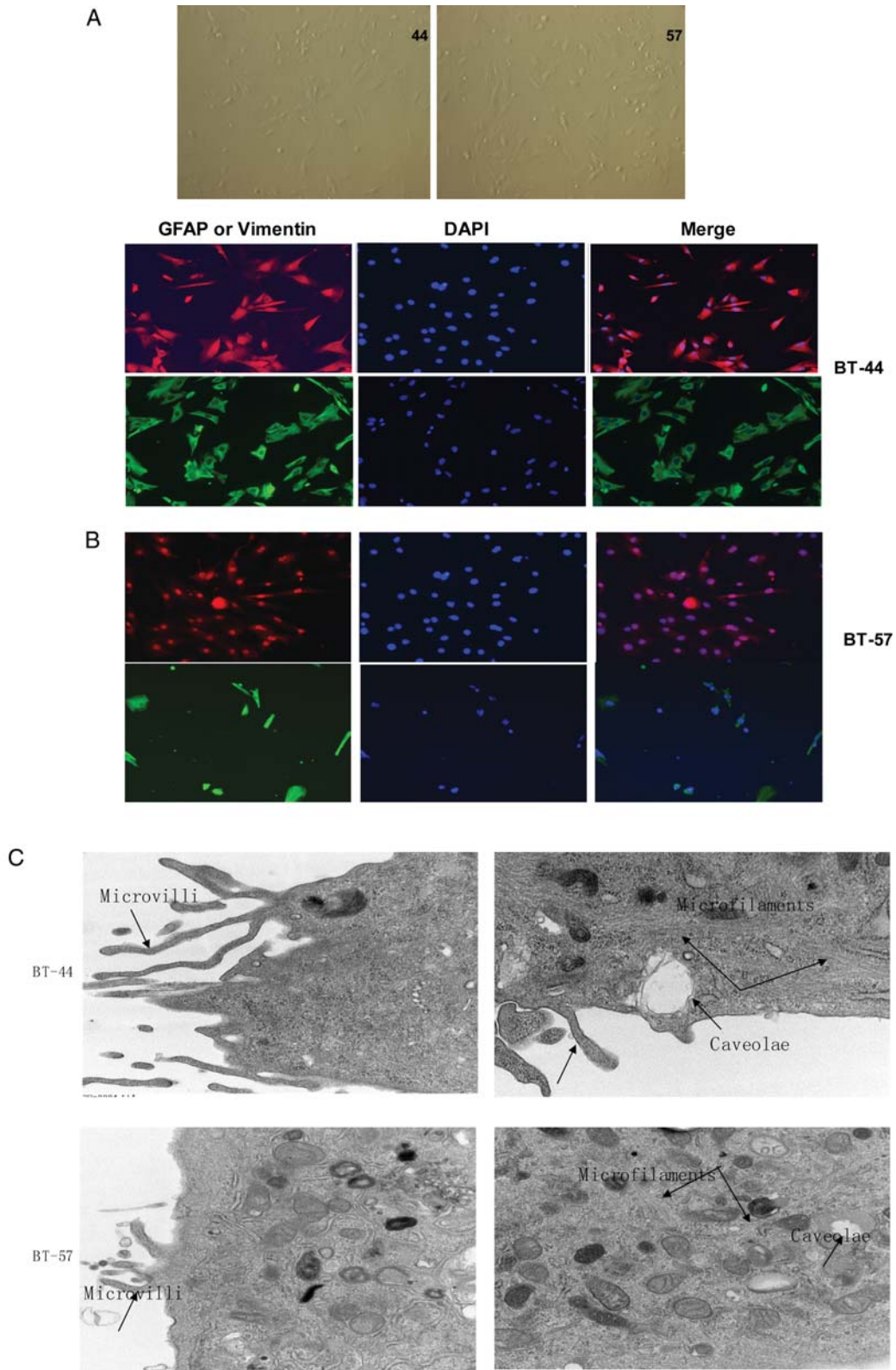


Fig. 3. Morphologic features of in vitro models. (A) Cells grown in vitro were evaluated to determine their morphologic features. Both BT-44 and BT-57 tumors had spindle-shaped cells. (B) BT-44 and BT-57 tumors showed positive staining results for glial fibrillary acidic protein (GFAP) and vimentin (top, BT-44; bottom, BT-57). (1) GFAP (red) or vimentin (green) staining. (2) DAPI staining. (3) A merged image of GFAP or vimentin and DAPI staining. (C) Ultrastructural features of ependymoma cells in culture. BT-44 and BT-57 tumors included numerous surface microvilli, many caveolae in the cytoplasm, and microfilaments (top, BT-44; bottom, BT-57). Direct magnification: 25 000.

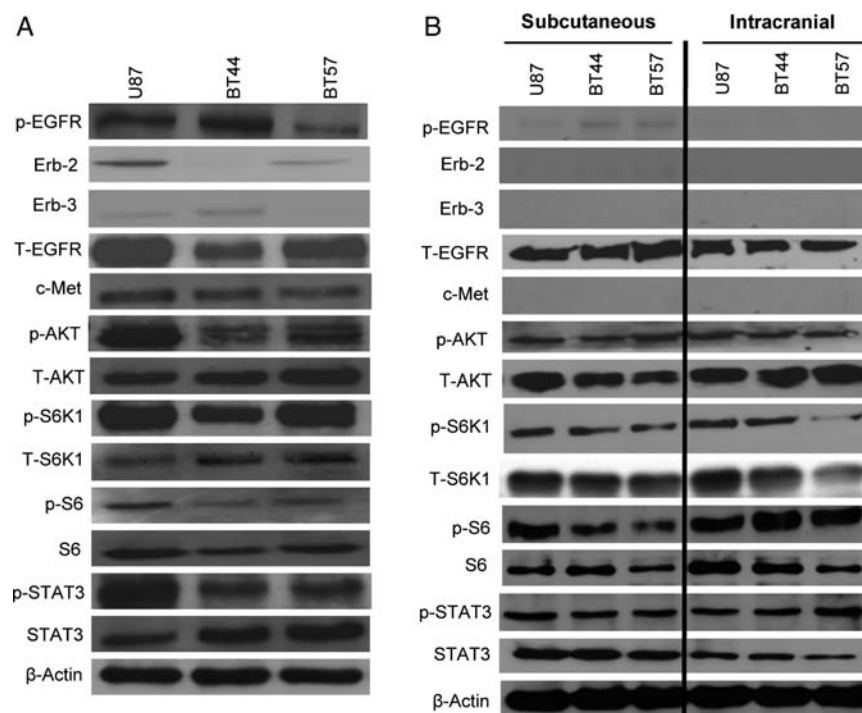


Fig. 4. Expression profile of ependymoma cells and tumor tissues. (A) BT-44 and BT-57 protein extracts were evaluated using Western blot analysis and different signaling antibodies, as described in Materials and Methods. For all the antibodies cells were grown in growth media as described in Materials and Methods, however to detect pEGFR, cells were starved for 24 h and stimulated with 100 ng/mL EGF for 30 min to look for EGFR activation.

concentration-dependent manner in association with treatment with these drugs (Fig. 5A). Temozolomide (0.4 mM) and carboplatin (30  $\mu$ g/mL) were sufficient to significantly decrease ependymoma cell proliferation, as measured by the CTB assay in all cell lines studied.

#### *NVP-BEZ-235: a PI3 K Inhibitor Blocks Activation of PI3K-Mediated Signaling in Ependymoma*

In this study, we evaluated the effects of NVP-BEZ-235 on PI3K signaling in ependymoma cells in vitro. Treatment of BT-44 and BT-57 cells with NVP-BEZ-235 blocked both the basal and EGF-induced phosphorylation of Akt at concentrations as low as 5–10 nM (Fig. 5B). NVP-BEZ235 also reduced the activation of intracellular Akt downstream targets, including pS6. However, NVP-BEZ235 did not inhibit basal and EGF-induced MAPK activation, suggesting that NVP-BEZ235 selectively blocks the PI3K/Akt pathway in ependymoma cell lines.

#### *Erlontinib: a EGFR Inhibitor Inhibits EGFR-Mediated Signaling in Ependymoma*

As shown in Fig. 5C, increasing doses of erlontinib resulted in reduction in the levels of phosphorylated EGFR, whereas the amount of total EGFR did not change significantly with drug treatment. EGFR promotes cellular proliferation and resistance to apoptotic stimuli through intracellular mediators, including ERK

and Akt. Akt phosphorylation levels induced in response to EGF treatment were decreased in association with treatment with erlontinib (Fig. 5C). ERK phosphorylation was less clearly induced by EGF treatment and only decreased by erlontinib at the highest doses, suggesting that ERK activation may not depend on EGFR in these ependymoma models.

## Discussion

Ependymomas are tumors that arise in the CNS. Little is known about the aberrant cellular and molecular processes that generate these tumors, and this lack of knowledge has hampered efforts to reduce the significant mortality and morbidity rates of the disease. Thus, a disease model is needed to understand ependymoma's biological characteristics.

Few experimental models of ependymoma have been described in contrast to other brain tumors. Thus far, to our knowledge, only 2 ependymoma cell lines have been developed. In one study, cells were cultured up to 4 passages;<sup>24</sup> and in the other study, a relatively complicated coculture of an ependymoma cell line was established.<sup>25</sup> In addition, the National Cancer Institute supported Pediatric Preclinical Testing Program has systematically evaluated new agents against molecularly characterized childhood solid tumors and has used the BT-44 xenograft line in various drug testings.<sup>13–17</sup> Recently, Yu et al<sup>18</sup> described the establishment of a clinically relevant mouse model of ependymoma and a

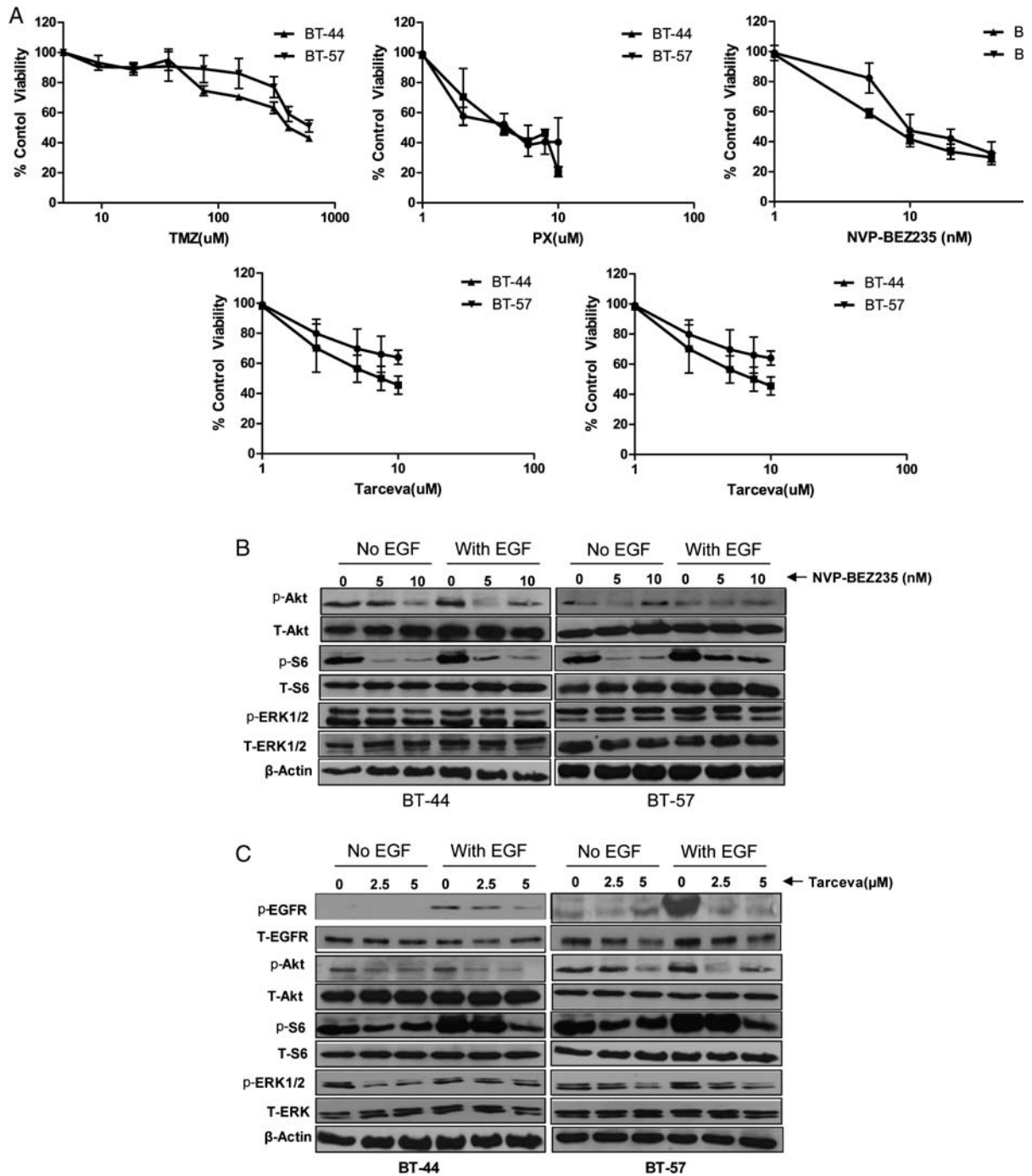


Fig. 5. Inhibitor treatment inhibited ependymoma cell proliferation. (A) Ependymoma cells in 96-well plates were treated with increasing concentrations of different inhibitors for 72 h and subjected to a CTB assay, as described in Materials and Methods. The plot depicts the percentage growth of treated cells compared with the growth of vehicle-treated control cells. Each culture was performed in triplicate. The results shown are the arithmetic mean  $\pm$  the standard deviation from a single experiment. (B) Effect of NVP-BEZ235 and erlotinib on signal transduction pathways. Western blot analysis of BT-44 and BT-57 ependymoma models were performed as follows: Cells were serum-starved for 24 h and treated with different concentrations of NVP-BEZ235 and erlotinib, as described in Materials and Methods. Cells were either left starved or stimulated with epidermal growth factor (100 ng/mL) for 10 min before harvest. The results show that NVP-BEZ235 and erlotinib both inhibited phosphorylation of Akt at Ser-473 without modifying levels of total Akt protein (T-Akt). Equal loading was confirmed by immunoblotting with anti-actin antibody. Data shown are a representative immunoblot of three independent experiments.

permanent cell line that was passaged  $\geq 70$  times. In the present study, we successfully established 2 in vitro and 2 in vivo ependymoma xenografts (BT-44 and BT-57)

derived from primary tumors. Establishing an in vitro model is more challenging than establishing an in vivo model, particularly in separating cells, controlling for



microenvironment alterations, and adequate nutritional requirements. To overcome these hindrances, we used poly-D lysine-coated flasks, which resulted in the best attachment conditions for suspended cells, and we used additional growth factors (eg, EGF and basic fibroblast growth factor) to accelerate cell growth. GFAP is an intermediate filament protein that is thought to be specific for astrocytes in the CNS.<sup>26–28</sup> It is also expressed by other cell types in CNS ependymal cells. Vimentin, which makes up the cytoskeleton, is another member of the intermediate filament family of proteins.<sup>27</sup> GFAP and vimentin were both expressed in our ependymoma cell lines and could be useful as markers of ependymoma. Electron microscopy revealed the ultrastructural characteristics of ependymoma, such as intermediate microfilaments and numerous surface microvilli and caveolae. All of these characteristics demonstrated our success in establishing 2 *in vitro* and 2 *in vivo* models of ependymoma (BT-44 and BT-57).

The *in vivo* subcutaneous model showed exponential growth of tumor mass, and intracranial tumors in nude mice invaded in brain parenchyma. The most typical histologic feature of ependymoma, pseudorosettes,<sup>2</sup> was found in all tumor samples; pseudorosettes are a pathologic diagnostic marker of ependymoma, according to the WHO classification system. Ki-67 protein expression in proliferating cells<sup>29</sup> has previously been reported as a prognostic factor in pediatric ependymoma.<sup>30,31</sup> In the present study, a Ki-67 index (>10%) indicated a medium proliferation rate in intracranial xenografts. Subcutaneous tumors had lower Ki-67 expression than did intracranial tumors, demonstrating a lower proliferation rate. It is highly possible that changes in the tumor growth microenvironment attenuate tumor growth.

Surgery has an established role in the treatment and clinical outcome of ependymoma, but the value of adjuvant chemotherapy and radiotherapy is less clear.<sup>11,32–36</sup> Tumorigenic signal pathways may serve as cellular targets for novel therapeutic approaches. However, the biological characteristics of ependymomas are largely unknown, mainly because they are heterogeneous: patients can be categorized into a wide range of subgroups on the basis of the tumor's histological characteristics and localization, resulting in relatively small series of patients. An important recent finding is that gene expression signatures of ependymomas from different locations of the CNS are correlated with those of the corresponding region of the normal developing CNS.<sup>37</sup> The differentially expressed genes are predominantly involved in regulating neural precursor cell proliferation and differentiation. Several studies have evaluated the receptor tyrosine kinase I family in ependymoma. Coexpression of ERBB2/ERBB4, in association with

Ki-67 expression and the degree of surgical resection required, were found to be associated with more aggressive disease behavior.<sup>29</sup> In another study, high EGFR protein expression in intracranial ependymomas was correlated with poor prognosis in a univariate analysis, whereas multivariate analysis revealed that EGFR overexpression was the only significant factor in grade II tumors.<sup>38</sup> BT-44 xenografts have been earlier used by various investigators for various preclinical tests, and recently, Carol et al<sup>39</sup> used an Akt inhibitor GSK690693 to evaluate the anti-tumor activity of this agent. We also tested the altered molecular signaling patterns in ependymoma models and found aberrant activation of the PI3K, ERK, and EGFR signaling pathways. Recently, more and more research has focused on the stem cell-like characteristics of ependymoma.<sup>40–42</sup> In 2005, Poppleton and Gilbertson<sup>40</sup> reported that radial glia cells are candidate stem cells of ependymoma. The Notch cell signaling pathway and the HOX family of transcription factors are involved in the stem cell phenotype in ependymoma. Sanai et al<sup>43</sup> found that in the adult human brain, neural stem cells were GFAP positive. These findings support the use of treatment strategies that focus on eradicating ependymoma cancer stem cells.

In conclusion, the human ependymoma models established in our study could be useful for understanding the key molecular pathways identified in proteomic analyses and to screen targeted therapeutic strategies.

## Acknowledgments

We thank Ann M. Sutton (Department of Scientific Publications, The University of Texas MD Anderson Cancer Center) for editing the manuscript. We thank Verlene Henry and Lindsay Homes for animal studies.

*Conflict of interest statement.* None declared.

## Funding

This study was supported by funds from the Collaborative Ependymoma Research Network (CERN) foundation and also funds from Childrens Brain Tumor Foundation grant to D.K. We acknowledge assistance from Institutional Core Grant #CA16672, which was awarded to the High Resolution Electron Microscopy Facility, The University of Texas MD Anderson Cancer Center.

## References

1. Oppenheim JS, Strauss RC, Mormino J, Sachdev VP, Rothman AS. Ependymomas of the third ventricle. *Neurosurgery*. 1994;34:350–352.
2. Godfraind C. Classification and controversies in pathology of ependymomas. *Childs Nerv Syst*. 2009;25(10):1185–1193.

3. Bouffet E, Perilongo G, Canete A, Massimino M. Intracranial ependymomas in children: a critical review of prognostic factors and a plea for cooperation. *Med Pediatr Oncol.* 1998;30:319–329.
4. Robertson PL, Zeltzer PM, Boyett JM, et al. Survival and prognostic factors following radiation therapy and chemotherapy for ependymomas in children: a report of the Children's Cancer Group. *J Neurosurg.* 1998;88:695–703.
5. Horn B, Heideman R, Geyer R, et al. A multi-institutional retrospective study of intracranial ependymoma in children: identification of risk factors. *J Pediatr Hematol Oncol.* 1999;21:203–211.
6. Grill J, Le Deley MC, Gambarelli D, et al. Postoperative chemotherapy without irradiation for ependymoma in children under 5 years of age: a multicenter trial of the French Society of Pediatric Oncology. *J Clin Oncol.* 2001;19:1288–1296.
7. Schiffer D, Giordana MT. Prognosis of ependymoma. *Childs Nerv Syst.* 1998;14:357–361.
8. Needle MN, Goldwein JW, Grass J, et al. Adjuvant chemotherapy for the treatment of intracranial ependymoma of childhood. *Cancer.* 1997;80:341–347.
9. McGuire CS, Sainani KL, Fisher PG. Both location and age predict survival in ependymoma: a SEER study. *Pediatr Blood Cancer.* 2009;52:65–69.
10. Packer RJ. Ependymomas in children. *J Neurosurg.* 2000;93:721–723.
11. Kano H, Niranjana A, Kondziolka D, Flickinger JC, Lunsford LD. Outcome predictors for intracranial ependymoma radiosurgery. *Neurosurgery.* 2009;64:279–287.
12. Gottesman MM, Pastan I. Biochemistry of multidrug resistance mediated by the multidrug transporter. *Annu Rev Biochem.* 1993;62:385–427.
13. Vassal G, Merlin JL, Terrier-Lacombe MJ, et al. In vivo antitumor activity of S16020, a topoisomerase II inhibitor, and doxorubicin against human brain tumor xenografts. *Cancer Chemother Pharmacol.* 2003;51:385–394.
14. Middlemas DS, Stewart CF, Kirstein MN, et al. Biochemical correlates of temozolomide sensitivity in pediatric solid tumor xenograft models. *Clin Cancer Res.* 2000;6:998–1007.
15. Mintz MB, Sowers R, Brown KM, et al. An expression signature classifies chemotherapy-resistant pediatric osteosarcoma. *Cancer Res.* 2005;65:1748–1754.
16. Bachmann PS, Gorman R, Mackenzie KL, Lutze-Mann L, Lock RB. Dexamethasone resistance in B-cell precursor childhood acute lymphoblastic leukemia occurs downstream of ligand-induced nuclear translocation of the glucocorticoid receptor. *Blood.* 2005;105:2519–2526.
17. Houghton PJ, Adamson PC, Blaney S, et al. Testing of new agents in childhood cancer preclinical models: meeting summary. *Clin Cancer Res.* 2002;8:3646–3657.
18. Yu L, Baxter PA, Voicu H, et al. A clinically relevant orthotopic xenograft model of ependymoma that maintains the genomic signature of the primary tumor and preserves cancer stem cells in vivo. *Neuro Oncol.* 2010;12(6):580–594.
19. Lal S, Lacroix M, Tofilon P, et al. An implantable guide-screw system for brain tumor studies in small animals. *J Neurosurg.* 2000;92:326–333.
20. Gentile V, Vicini P, Giacomelli L, et al. Detection of human papillomavirus DNA, p53 and ki67 expression in penile carcinomas. *Int J Immunopathol Pharmacol.* 2006;19:209–215.
21. Alvarez JI, Teale JM. Breakdown of the blood brain barrier and blood-cerebrospinal fluid barrier is associated with differential leukocyte migration in distinct compartments of the CNS during the course of murine NCC. *J Neuroimmunol.* 2006;173:45–55.
22. Koul D, Jasser SA, Lu Y, et al. Motif analysis of the tumor suppressor gene MMAC/PTEN identifies tyrosines critical for tumor suppression and lipid phosphatase activity. *Oncogene* 2002;21:2357–2364.
23. Skehan P, Storeng R, Scudiero D, et al. New colorimetric cytotoxicity assay for anticancer-drug screening. *J Natl Cancer Inst.* 1990;82:1107–1112.
24. Jennings MT, Kaariainen IT, Gold L, Maciunas RJ, Commers PA. TGF beta 1 and TGF beta 2 are potential growth regulators for medulloblastomas, primitive neuroectodermal tumors, and ependymomas: evidence in support of an autocrine hypothesis. *Hum Pathol.* 1994;25:464–475.
25. Brisson C, Lelong-Rebel I, Mottolese C, et al. Establishment of human tumoral ependymal cell lines and coculture with tubular-like human endothelial cells. *Int J Oncol.* 2002;21:775–785.
26. Tardy M, Fages C, Le Prince G, Rolland B, Nunez J. Regulation of the glial fibrillary acidic protein (GFAP) and of its encoding mRNA in the developing brain and in cultured astrocytes. *Adv Exp Med Biol.* 1990;265:41–52.
27. Fuchs E, Weber K. Intermediate filaments: structure, dynamics, function, and disease. *Annu Rev Biochem.* 1994;63:345–382.
28. Bongcam-Rudloff E, Nister M, Betsholtz C, et al. Human glial fibrillary acidic protein: complementary DNA cloning, chromosome localization, and messenger RNA expression in human glioma cell lines of various phenotypes. *Cancer Res.* 1991;51:1553–1560.
29. Gerdes J, Lemke H, Baisch H, et al. Cell cycle analysis of a cell proliferation-associated human nuclear antigen defined by the monoclonal antibody Ki-67. *J Immunol.* 1984;133:1710–1715.
30. Gilbertson RJ, Bentley L, Hernan R, et al. ERBB receptor signaling promotes ependymoma cell proliferation and represents a potential novel therapeutic target for this disease. *Clin Cancer Res.* 2002;8:3054–3064.
31. Bennetto L, Foreman N, Harding B, et al. Ki-67 immunolabelling index is a prognostic indicator in childhood posterior fossa ependymomas. *Neuropathol Appl Neurobiol.* 1998;24:434–440.
32. Wright KD, Gajjar A. New chemotherapy strategies and biological agents in the treatment of childhood ependymoma. *Childs Nerv Syst.* 2009;25(10):1275–1282.
33. Merchant TE, Li C, Xiong X, Gaber MW. Cytokine and growth factor responses after radiotherapy for localized ependymoma. *Int J Radiat Oncol Biol Phys.* 2008;74(1):159–167.
34. Peres E, Wood GW, Poulik J, et al. High-dose chemotherapy and adoptive immunotherapy in the treatment of recurrent pediatric brain tumors. *Neuropediatrics.* 2008;39:151–156.
35. Packer RJ. Childhood brain tumors: accomplishments and ongoing challenges. *J Child Neurol.* 2008;23:1122–1127.
36. Goldhoff P, Warrington NM, Limbrick DD, Jr., et al. Targeted inhibition of cyclic AMP phosphodiesterase-4 promotes brain tumor regression. *Clin Cancer Res.* 2008;14:7717–7725.
37. Taylor MD, Poppleton H, Fuller C, et al. Radial glia cells are candidate stem cells of ependymoma. *Cancer Cell.* 2005;8:323–335.
38. Mendrzyk F, Korshunov A, Benner A, et al. Identification of gains on 1q and epidermal growth factor receptor overexpression as independent prognostic markers in intracranial ependymoma. *Clin Cancer Res.* 2006;12:2070–2079.
39. Carol H, Morton CL, Gorlick R, et al. Initial testing (stage 1) of the Akt inhibitor GSK690693 by the pediatric preclinical testing program. *Pediatr Blood Cancer.* 2010;55(7):1329–1337. doi: 10.1002/pbc.22710. Epub 2010 Aug 25.

40. Poppleton H, Gilbertson RJ. Stem cells of ependymoma. *Br J Cancer*. 2007;96:6–10.
41. de Bont JM, Packer RJ, Michiels EM, Boer ML, Pieters R. Biological background of pediatric medulloblastoma and ependymoma: a review from a translational research perspective. *Neuro Oncol*. 2008;10:1040–1060.
42. Nicolis SK. Cancer stem cells and “stemness” genes in neuro-oncology. *Neurobiol Dis*. 2007;25:217–229.
43. Sanai N, Tramontin AD, Quinones-Hinojosa A, et al. Unique astrocyte ribbon in adult human brain contains neural stem cells but lacks chain migration. *Nature*. 2004;427:740–744.